



The Incorporation of a Discrete, Dynamic LTC Transformer Model in a Dynamic Power Flow Algorithm

Garcia-Valle, Rodrigo; Acha, Enrique

Published in:

The International Association of Science and Technology for Development

Publication date:

2007

[Link back to DTU Orbit](#)

Citation (APA):

Garcia-Valle, R., & Acha, E. (2007). The Incorporation of a Discrete, Dynamic LTC Transformer Model in a Dynamic Power Flow Algorithm. In *The International Association of Science and Technology for Development* Acta Press.

General rights

Copyright and moral rights for the publications made accessible in the public portal are retained by the authors and/or other copyright owners and it is a condition of accessing publications that users recognise and abide by the legal requirements associated with these rights.

- Users may download and print one copy of any publication from the public portal for the purpose of private study or research.
- You may not further distribute the material or use it for any profit-making activity or commercial gain
- You may freely distribute the URL identifying the publication in the public portal

If you believe that this document breaches copyright please contact us providing details, and we will remove access to the work immediately and investigate your claim.

THE INCORPORATION OF A DISCRETE, DYNAMIC LTC TRANSFORMER MODEL IN A DYNAMIC POWER FLOW ALGORITHM

Rodrigo Garcia-Valle

Department of Electronics and Electrical Engineering
University of Glasgow
Glasgow, UK
email: r.garcia@elec.gla.ac.uk

Enrique Acha

Department of Electronics and Electrical Engineering
University of Glasgow
Glasgow, UK
email: e.acha@elec.gla.ac.uk

ABSTRACT

This paper reports on the development of a dynamic LTC transformer model suitable for a dynamic power flow algorithm where the generators dynamic equations are solved simultaneously and in conjunction with the network algebraic equations using Newton's method. The method may be used for long-term power systems dynamic assessment, and in addition to the load tap changing transformer model, a representation of the generator boiler is also included. These are slow acting devices which are known to impact on system voltage collapse phenomena; events which may evolve over periods of time lasting several tens of minutes. Two test systems are presented to show the versatility of the simulation tool, including a trip cascading event leading up to a wide-area voltage collapse. Where appropriate, result comparisons with the output of a conventional transient stability program have been carried out.

KEY WORDS

Dynamic power flows, voltage stability, dynamic stability, voltage collapse, LTC transformer, load shedding.

1 Introduction

Society's appetite for electricity continues unabated and with many transmission expansion programmes experiencing delays, existing transmission assets are being overstretched. Moreover, increased transmission system loadings and wide area disturbance propagation brought about by widespread interconnectivity, are calling for more accurate assessments of reactive power margins. On the main, power systems engineers have relied on the use of two kinds of application programs for bulk power systems assessments: power flows and transient stability. The former has been used to assess system voltage performance and active and reactive power flows and losses; all this from a snapshot of time perspective. Static power flows have been suitably extended to deal with voltage collapse assessment, with results normally provided in the form of P-V nose curves on the power-voltage plane. The approach yields a rather clear picture as to where the point of voltage collapse lies, as calculated by the static power flow solution. Nevertheless, it has been argued that the static approach incorporates no information about the dynamic behaviour of volt-

age collapse and that suitable elements of power systems dynamics should be included in the formulation. On the other hand, transient stability algorithms have traditionally been used to assess power systems dynamic phenomena from tens of milliseconds up to several seconds. These application programs include detailed models of synchronous generators with their excitation systems, turbines and governors; as well as dynamic models of loads and a wide range of power electronics-based converters. The voltage collapse phenomena is said to be dynamic in nature and yet when it presents itself, it normally does it in a manner that is rather slow when compared to the dynamic time frame of traditional transient stability programs. It is not uncommon for a voltage collapse event to evolve over a period of about 30 minutes; a time frame well beyond the intended scope of transient stability algorithms and models. Slow acting devices such as the time-dependent, discrete nature of load tap-changing transformer and boilers are not normally accounted for in transient stability programs and yet these slow acting devices together with the system load characteristic, have been reported [1] as having a direct bearing on the extent of a voltage collapse event.

Commensurate with industry's interest in achieving more realistic dynamic reactive power margins assessments, an existing solution approach [2] based on full time domain simulations is developed further in this paper. It is a unifying framework where the power flows representation of the network is combined with the dynamic models of the power system to enable combined solutions at pre-defined discrete time steps using the Newton-Raphson method. Such an approach is, in essence, a dynamic power flow method; a method that takes full account of all dynamic components in the power system, some of which may be non-linear and discontinuous in nature.

However, to enable comprehensive assessments of the many issues surrounding reactive power margins assessments and voltage collapse issues in today's power systems, fuller models of power plant components are required than those presented in [2]. Among these is the development of a dynamic LTC transformer with discrete taps. Where appropriate, the results reported in this paper are compared with the output of PSAT [3], a widely used transient stability simulation package within the academic community.

2 Dynamic power flows

The evolution of power flows in time, following an event, planned or unplanned, that alters a perceived steady-state of the network, may be tracked by suitably combining the dynamic equations of synchronous generators, loads and controls with the equations associated with a normal power flow solution:

$$0 = f(\mathbf{x}, \mathbf{y}) \quad (1)$$

$$\dot{\mathbf{y}} = g(\mathbf{y}, \mathbf{x}) \quad (2)$$

where \mathbf{y} and \mathbf{x} are vectors of integrable and non-integrable algebraic variables. Generally, f and g are non-linear vector functions and the non-integrable network variables cannot be eliminated algebraically. In such a situation, equations 1 and 2 must be solved simultaneously as a function of time [4]; where the possibility exists of using a unified framework to solve for \mathbf{y} and \mathbf{x} . The set 1 comprises network equations and the stator equations of synchronous machine, transformed into the network reference frame. Set 2 comprises the differential equations describing the synchronous generators and their controls.

2.1 Synchronous generator modelling

Three-phase synchronous generators represent the main source of electricity generation in interconnected power systems, where a key aspect of system operation is to maintain stable operation by running all synchronous generators at or near synchronous speed. However, power system disturbances, slowly-acting interactions between controls and emergency operations in the network may lead one or more generators in the network deviating from their intended synchronous speed. To a greater or lesser extent, all power systems dynamic problems involving synchronous generators require dynamic representation of their rotors, which may be in the form of their swing equations:

$$\dot{\omega} = \frac{\pi f_0}{H} [P_m - P_e - D(\omega - \omega_0)] \quad (3)$$

$$\dot{\delta} = \omega - \omega_0 \quad (4)$$

where H is the inertia constant, MW·s/MVA, P_m is the mechanical input power, p.u., P_e is the electrical output power, p.u., D is the damping coefficient, s/rad, ω is the synchronous speed, rad/s, f_0 is the system operating frequency, Hz and δ is the load angle, rad.

Assuming balanced operation and equipment, the set of equations that describe the dynamic behaviour of a salient-pole synchronous generator, in the dq plane, are:

$$T'_{d0} \dot{E}'_d = E_f + (X_d - X'_d)I_d - E'_q \quad (5)$$

$$T'_{q0} \dot{E}'_q = -E'_d - (X_q - X'_q)I_q \quad (6)$$

$$T''_{q0} \dot{E}''_d = E'_d + (X'_q - X''_q)I_q - E''_d \quad (7)$$

$$T''_{d0} \dot{E}''_q = E'_q + (X'_d - X''_d)I_d - E''_q \quad (8)$$

$$E'_q = V_q + R_a I_q + (X'_d - X_l)I_d \quad (9)$$

$$E'_d = V_d + R_a I_d - (X'_q - X_l)I_q \quad (10)$$

$$E''_q = V_q + R_a I_q + (X''_d - X_l)I_d \quad (11)$$

$$E''_d = V_d + R_a I_d - (X''_q - X_l)I_q \quad (12)$$

where T'_{d0} , T'_{q0} , T''_{d0} , T''_{q0} are open-circuit transient and sub-transient time constants in d and q axis, respectively. E'_d , E'_q , E''_d , E''_q , \dot{E}'_d , \dot{E}'_q , \dot{E}''_d , \dot{E}''_q are the internal transient and sub-transient flux voltages in d and q axis, and their time derivatives, respectively. E_f is the excitation (internal) voltage. V_d , V_q are generators terminal voltages in d and q axis, respectively. I_d , I_q , are the generators currents in d and q axis. X'_d , X'_q , X''_d , X''_q are transient and sub-transient reactances in d and q axis, respectively, X_d , X_q , are synchronous reactances in d and q axis, respectively, X_l is the leakage reactance, R_a is the armature resistance.

2.2 Network modelling

The basic equations representing the static part of the network are the active and reactive power injections at each network bus, say k :

$$P_k = e_k \sum_{m=1,n} (G_{km}e_m - B_{km}f_m) + \quad (13)$$

$$f_k \sum_{m=1,n} (G_{km}f_m + B_{km}e_m)$$

$$Q_k = f_k \sum_{m=1,n} (G_{km}e_m - B_{km}f_m) - \quad (14)$$

$$e_k \sum_{m=1,n} (G_{km}f_m + B_{km}e_m)$$

where P_k and Q_k are the active and reactive powers injected at bus k , e_k and f_k are the voltage's real and imaginary parts at bus k , G_{km} and B_{km} are the real and imaginary parts of the nodal admittance relating buses k and m . It should be noted that $k = m$ gives rise to the self admittance of bus k . Each plant component of the power network is represented by its own form of nodal admittance elements G_{kk} , B_{kk} , G_{km} and B_{km} .

2.3 Power transformer model

Power transformers are essential plant components of the power system. In addition to those that perform the basic functions of transforming an AC supply voltage into one or more different AC voltages and providing electrical insulation between the supply voltage and the user's equipment, there are transformers that are provided with an on-load tap changing mechanism to regulate voltage magnitude at a specified point of the network or to control the amount of active power that flows through the transformer. They are known as tap-changing and phase-shifting transformers, respectively. The equivalent circuit representation of a tap-changing transformer of impedance Z_l , with the tap mechanism T_k located on the primary side, and connected between buses k and m , is shown in Fig. 1.

The transfer admittance matrix for this equivalent circuit is:

$$\begin{pmatrix} Y_{kk} & Y_{km} \\ Y_{mk} & Y_{mm} \end{pmatrix} = \begin{pmatrix} Z_l^{-1} & -T_k Z_l^{-1} \\ -T_k Z_l^{-1} & T_k^2 Z_l^{-1} \end{pmatrix} \quad (15)$$

As indicated in Fig. 2 the transformer tap is discrete and updated according to the following relation:

$$T_k = V_{low} + \left(\frac{V_{high} - V_{low}}{T_{steps}} \right) T_{pos} \quad (16)$$

The tap's dynamic is represented by the following differential Equation:

$$\dot{T}_k = \frac{1}{H_T} \left(\sqrt{e_k^2 + f_k^2} - V_0 \right) \quad (17)$$

where H_T is the tap's servomotor inertia, e_k and f_k are the real and imaginary parts of the voltage at the regulated bus, V_0 is the target voltage magnitude.

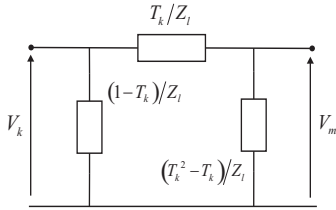


Figure 1. Tap-changing transformer equivalent circuit.

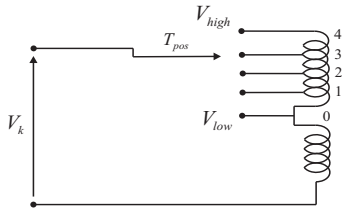


Figure 2. Transformer discrete tap.

3 Numerical Solution Technique

The set of algebraic and differential equations that describe each plant component of the power network are interdependent and it has been reported that their simultaneous calculation provides for a more stable numerical solution [2]. To this end, the system differential equations are transformed into algebraic equations and appended to the existing set of algebraic equations for a unified solution. One way of ensuring a numerically stable transformation is to use the implicit trapezoidal method, a technique known for giving reasonably accurate results even when relatively large integration time steps are selected [5].

The first step in the application of the trapezoidal method is to express the system differential equations in

the form of Equation 2. To exemplify the procedure, the method is applied to dynamic equations 3 and 4:

$$\omega_{(t)} - \omega_{(t-\Delta t)} = \frac{\Delta t}{2} \left[\frac{\pi f_0}{H} (P_m - P_{e(t)} - D(\omega_{(t)} - \omega_0)) + \frac{\pi f_0}{H} (P_m - P_{e(t-\Delta t)} - D(\omega_{(t-\Delta t)} - \omega_0)) \right] \quad (18)$$

$$\delta_{(t)} - \delta_{(t-\Delta t)} = \frac{\Delta t}{2} (\dot{\delta}_{(t)} + \dot{\delta}_{(t-\Delta t)}) \quad (19)$$

Substituting in Equation 18 the expression of electrical power P_e , where the effects of saliency and flux decay are considered, but assuming constant P_m , we have,

$$\begin{aligned} \omega_{(t)} - \omega_{(t-\Delta t)} = & \frac{\Delta t}{2} \left[\left(\frac{\pi f_0}{H} P_m \right. \right. \\ & + (E'_{d(t)} - R_a I_{d(t)} + (X'_q - X_l) I_{q(t)}) I_{d(t)} \\ & + (E'_{q(t)} - R_a I_{q(t)} + (X'_d - X_l) I_{d(t)}) I_{q(t)} \\ & \left. - D(\omega_{(t)} - \omega_0) \right) + \frac{\pi f_0}{H} (P_m \\ & + (E'_{d(t-\Delta t)} - R_a I_{d(t-\Delta t)} + (X'_q - X_l) I_{q(t-\Delta t)}) I_{d(t-\Delta t)} \\ & + (E'_{q(t-\Delta t)} - R_a I_{q(t-\Delta t)} + (X'_d - X_l) I_{d(t-\Delta t)}) I_{q(t-\Delta t)} \\ & \left. - D(\omega_{(t-\Delta t)} - \omega_0) \right) \right] \quad (20) \end{aligned}$$

Notice that in this Equation only the transient effects have been represented, as opposed to sub-transient ones, to keep the expression at a manageable level. Re-arranging terms, leads to a more compact expression,

$$F_\omega = F_{\omega(t)} + F_{\omega(t-\Delta t)} + C_\omega = 0 \quad (21)$$

$$F_\delta = F_{\delta(t)} + F_{\delta(t-\Delta t)} + C_\delta = 0 \quad (22)$$

where

$$F_{\omega(t)} = \omega_{(t)} + \frac{\Delta \pi f_0}{2H} (P_{e(t)} + D\omega_{(t)})$$

$$F_{\omega(t-\Delta t)} = -\omega_{(t-\Delta t)} + \frac{\Delta \pi f_0}{2H} (P_{e(t-\Delta t)} + D\omega_{(t-\Delta t)})$$

$$C_\omega = -\frac{\Delta t \pi f_0}{H} (P_m + D\omega_0)$$

Likewise, expression 19 is re-arranged,

$$F_{\delta(t)} = \delta_{(t)} - \frac{\Delta t}{2} \omega_{(t)}$$

$$F_{\delta(t-\Delta t)} = -\delta_{(t-\Delta t)} - \frac{\Delta t}{2} \omega_{(t-\Delta t)}$$

$$C_\delta = 2\pi f_0 \Delta t$$

Equations 13 and 14, describing the active and reactive powers injected in the network buses, are augmented to incorporate explicitly the active and reactive powers contributed by all generators in the network. Hence,

$$\begin{aligned} P_{(k)} + P_{e(\text{genbus}(l))} \\ Q_{(k)} + Q_{e(\text{genbus}(l))} \end{aligned} \quad (23)$$

for $k=1, \dots, n_{\text{bus}}$ and $l=1, \dots, n_{\text{gen}}$, where $\text{genbus}(l)$ is an array of generator-connected buses.

Equations 13-14 for load buses and Equations 21-22 for generator buses form the necessary set with which to carry out dynamic power flow solutions of a power system. One option to achieve this is to solve the equation set, which is non-linear, using the Newton-Raphson method. Hence, the following linearised equation, around a base point, provides the computing engine with which to carry out the solution by iteration:

$$\begin{bmatrix} \Delta P \\ \Delta Q \\ \dots \\ F_\omega \\ F_\delta \\ F_{E'_d} \\ F_{E'_q} \\ F_{E''_d} \\ F_{E''_q} \end{bmatrix} = \begin{bmatrix} J_{11} & | & J_{12} \\ \dots & + & \dots \\ J_{21} & | & J_{22} \end{bmatrix} \begin{bmatrix} \Delta e \\ \Delta f \\ \dots \\ \Delta \omega \\ \Delta \delta \\ \Delta E'_d \\ \Delta E'_q \\ \Delta E''_d \\ \Delta E''_q \end{bmatrix} \quad (24)$$

Where J_{11} is a matrix of first order partial derivatives of the active and reactive power, P and Q , with respect to nodal voltages, e, f . The active and reactive powers contributed by the generators are taken into consideration in the Jacobian term, J_{11} . J_{22} is a matrix of partial derivatives of generators discretised functions of the form 21 and 22, with respect to generator state variables $\omega, \delta, E'_d, E'_q, E''_d$ and E''_q . J_{12} is a matrix of first order partial derivatives of active and reactive power at generator buses with respect to generator state variables. J_{21} is a matrix of first order partial derivatives of generator discretised functions of the form 21 and 22, with respect to nodal voltages e, f .

It should be remarked that in Equation 24 the mechanical power P_m contributed by the boiler-turbine-governor set has been taken to remain constant, for the sake of simplifying the equation. In practice, however, the boiler-turbine-governor set is an important dynamic element in power systems long term dynamics and the linearised Equation 24 may be suitably expanded to accommodate the boiler-turbine-governor representation.

4 Results

4.1 Validation

To validate the solution technique, a time domain simulation has been carried out and compared with PSAT [3]. The test system used is the nine-bus, three-machine power system depicted at Fig. 3 [6]. The scenario considered for this study is a load change at bus 8. A load of 10MW is added at $t = 1m$, using a 10 p.u. resistive impedance. The simulation is run for five seconds. It should be noted from Fig. 4 and Fig. 5, that the system response at Bus 1, is more damped than those at Buses 2 and 3. This is due to the fact that these two buses are closer to the perturbation point. Fig. 6 presents the machines angle responses. It is noted that the angular differences of the machines are small, thus, the system will remain stable after the disturbance. The simulation results provided by

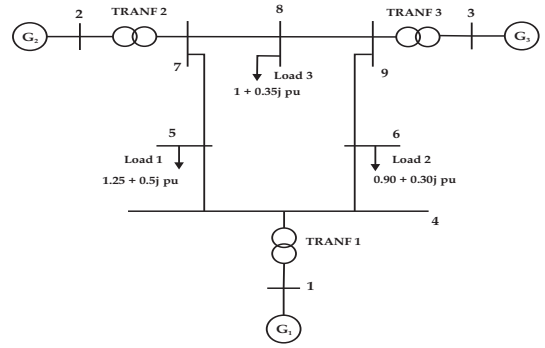


Figure 3. 3 Machines 9 buses power system.

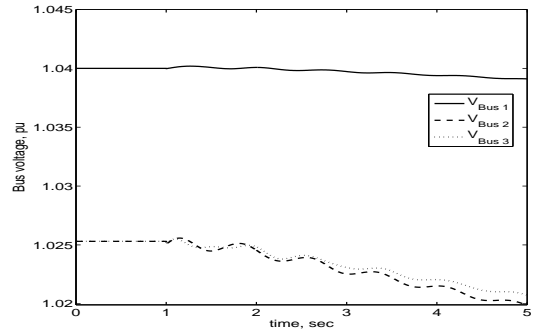


Figure 4. Bus voltage response to a load change.

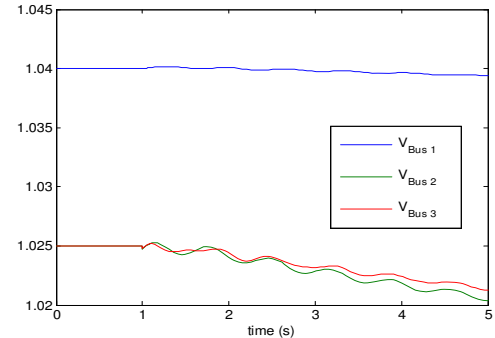


Figure 5. PSAT output for bus voltage response to a load change.

the dynamic power flow simulation agree on well with the response provided by PSAT, Fig. 5.

4.2 Test Case 1

To demonstrate the applicability and versatility of the dynamic power flow computer program, the load connected at bus 8 is increased by 50%. All loads are represented by their exponential load model [7]. The simulation period is 25 minutes.

Fig. 7 represents the system with a mechanical power

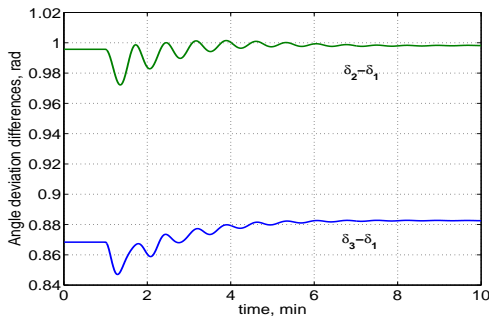


Figure 6. $\delta_i - \delta_1$ response to the load change.

P_m constant, dash line, whereas the continuous line represents the mechanical power associated with the boiler-turbine-governor set model.

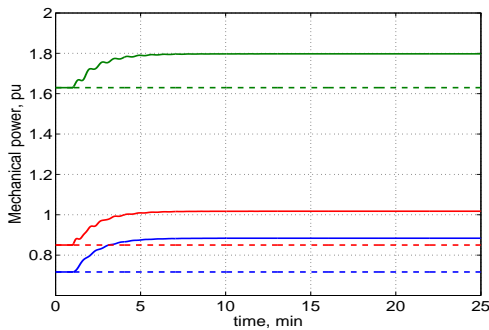


Figure 7. Synchronous generators' mechanical power.

4.3 Test Case 2

To assess the performance of the Dynamic Load Tap-Changer (DLTC) model, a separate test case is carried out. A load increment in bus 8 is used as the source of the perturbation. Fig. 8 shows the DLTC performance following the perturbation. Dynamic tap-changers 2 and 3 are closer to the perturbation point and their action is more pronounced than dynamic tap-changer 1 which is farther away; it is noted that after an initial drop, it returns to a value closer to its pre-disturbance value. Fig. 9 gives the voltage profiles at buses where the load tap changers are connected to. When the load tap changer is active, 'ON', given by the continuous line, and when the load tap changer is inactive, 'OFF', given by the dashed line. In this test case, the dynamic load tap changer plays a very important role in improving the voltage profile at these specific points of the system. However, this may be at the expenses of a temporary surge in reactive power consumption from the network, as shown in Fig. 10.

4.4 Test Case 3

To show the wider applicability of the proposed approach, the New England system [8] depicted in Fig. 11, is used. The system has been modified to include one tap-changing transformer between buses 40 and 3.

At first, transmission lines which connect bus 17 with buses 27, 16 and 18 are tripped; as a consequence bus 17 including its load, is isolated from the system, producing a voltage drop at the majority of nodes. Next, the transmission line connecting buses 3 and 18 is taken out of service, causing that node 18 and its load become separated from the system, bringing a recovery of system voltages. This is followed by a tripping of the transmission line connecting buses 3 to 4; an event that triggers a voltage collapse of the entire system.

Fig. 12 shows the voltage magnitudes in the remaining 37 buses of the system. Fig. 13 shows the discrete response of the tap-changer under abrupt voltage changes. It can be seen that this device works in its pre-specified working range, which is from 0.90 to 1.10. The tap changer performance can be observed in Fig. 13. Fig. 14 shows the voltage profile at the bus where the voltage is controlled by the tap-changer. As shown, the tap-changer transformer is able to control the voltage around its specified value, 1 p.u., even when the system is undergoing unfavourable conditions.

5 Conclusions

This paper presents a unified framework for dynamic simulations, where the application of the trapezoidal rule and Newton-Raphson technique are applied to solve the combined system. The trapezoidal rule is applied to discretise the synchronous machines variable and the dynamic equations corresponding to the DLTC. A detailed mathematical modelling for the synchronous generator is presented.

The solution technique is validated, obtaining acceptable accuracy results. The New England power system has been tested and subjected to this approach getting good results.

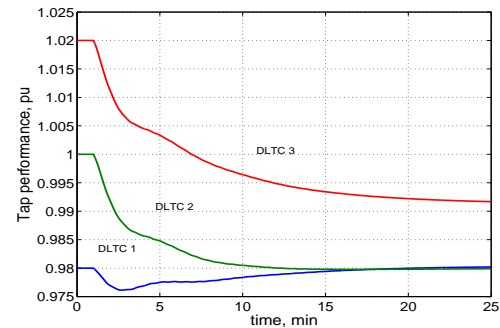


Figure 8. Dynamic Load Tap-Changer (DLTC) performance.

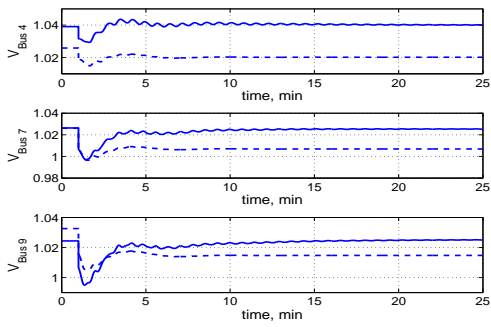


Figure 9. Voltage magnitude at Buses 4, 7 and 9, tap changer ON (—) and tap changer OFF (---).

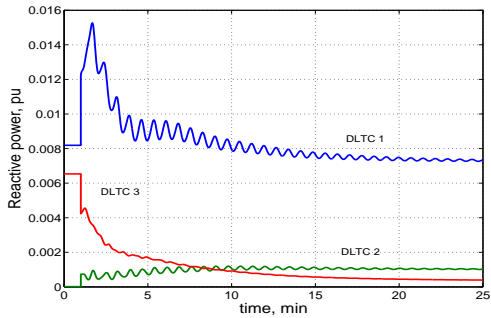


Figure 10. Reactive power consumption of the Dynamic Load Tap-Changer (DLTC).

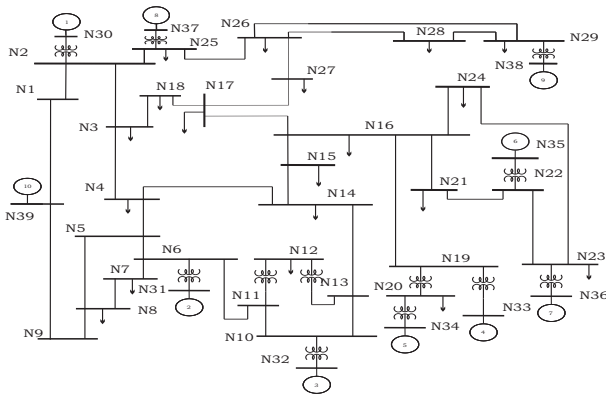


Figure 11. One-line New England test system diagram.

References

[1] IEEE Power Engineering Society, "Voltage Stability Assessment: Concepts, Practices and Tools", Final document," August 2002.

[2] M. Rafian, M. J. H. Sterling, and M. R. Irving, "Real-time power system simulation," *IEE Proceedings*, vol. 134, no. 3, pp. 209–223, May 1987.

[3] F. Milano, "An open source power system analysis toolbox," *IEEE Transaction, Power Systems*, vol. 20,

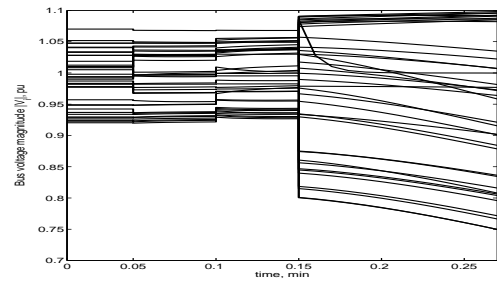


Figure 12. Bus voltages' response.

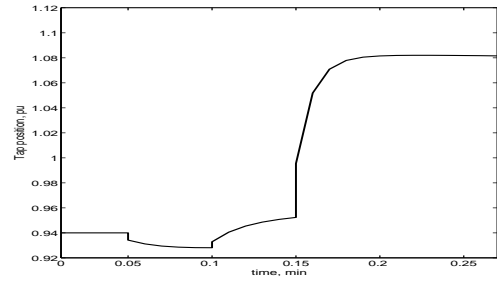


Figure 13. Dynamic load tap changer performance.

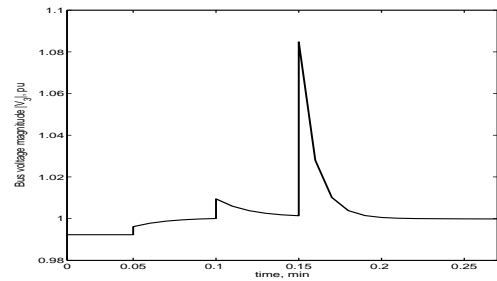


Figure 14. Voltage magnitude at Bus 3.

pp. 1199–1206, August 2005.

[4] C. W. Gear, "Simultaneous numerical solution of differential-algebraic equations," *IEEE Transactions Circuit Theory*, vol. 18, pp. 89–95, January 1971.

[5] J. Machowski, J. W. Bialek, and J. R. Bumby, *Power System Dynamic and Stability*. John Wiley & Sons, Inc., 1997.

[6] P. M. Anderson and A. A. Fouad, *Power System Control and Stability*. IEEE Press, 1997.

[7] IEEE Task Force on Load Representation, "Bibliography on load models for power flow and dynamic performance simulation," *IEEE Transaction on Power Systems*, vol. 10, pp. 523–538, February 1995.

[8] J. H. Chow, *Time-Scale Modeling of Dynamic Networks with Applications to Power Systems*. Springer-Verlag, 1982.